Effect of Accelerating Methods on Gas Nitriding

Subjects: Metallurgy & Metallurgical Engineering

Contributor: Zhi-Wei Li, Yu-Long Zhou, Fan Xia, Ai-Jun Xie, Hao-Ping Peng, Jian-Hua Wang

Gas nitriding, as a surface modification technology to improve the wear resistance of workpiece surfaces, is widely used in wind turbine gears, pressure vessel gears, high-precision die casting abrasives, and other areas. However, the gas nitriding time is too long, reaching 40–60 h, which reduces the efficiency of nitriding and hinders the development of gas nitriding. Therefore, various accelerating methods are born accordingly. There are five common accelerating methods are summarized: process parameter optimization, surface mechanical nano-crystallization, surface-active catalysis, surface pre-oxidation, and surface laser treatment.

Keywords: gas nitriding ; accelerating methods ; nitriding behavior

1. Introduction

Gas nitriding is a chemical heat treatment process which makes nitrogen atoms penetrate into the surface of the workpiece at a certain temperature and in a certain medium [1][2]. It generally includes three processes [3][4][5]: generation of active nitrogen atoms, surface absorption, and diffusion of nitrogen atoms. The surface of the workpiece after nitriding treatment usually has the characteristics of high hardness [6], good wear resistance [7], high fatigue strength [8], and excellent corrosion resistance [1]. However, the traditional nitriding temperature is high and the nitriding time is long, which not only wastes energy and increases the manufacturing cost of the workpiece but also causes some performance reduction in the workpiece. For example, if the nitriding temperature of stainless steel is too high, it will cause a lack of chromium in the substrate and the degradation of corrosion resistance [9][10][11][12]. For aluminum alloy workpieces, if the nitriding temperature is too high, the matrix structure will change significantly, which will lead to poor inherent properties [13][14]. In the nitriding process, the temperature affects the nitriding speed, the decomposition efficiency of the nitriding medium, and the structure of the nitrided layer [15][16]. CrMo steel is usually used to manufacture parts with high strength and high-temperature operation, such as boilers, pressure vessels, steam turbine components, etc. Gas nitriding can improve the hardness and wear resistance of CrMo steel, making it more suitable for use in high-stress and high-temperature environments. It can also improve the corrosion resistance and prolong the life of the parts. Nickel-based alloys are widely used in high-temperature and corrosive environments, such as the aerospace, petrochemical, and energy industries. Gas nitriding can improve the surface hardness and wear resistance of nickel-based alloys and improve their performance in high-temperature and corrosive environments. This helps to extend the service life of alloy parts. Cobalt-based alloys are commonly used in the manufacture of high-temperature, high-strength, and corrosion-resistant parts, such as aero-engine parts and chemical equipment. Gas nitriding can increase the hardness and wear resistance of cobalt-based alloys and improve their stability in high-temperature and corrosive environments. This is very important for extending the life of alloy parts. Cemented carbides are commonly used for cutting, drilling, grinding, and other cutting tools as well as wear-resistant parts, such as mechanical seals and bearings. Gas nitriding can increase the surface hardness and wear resistance of cemented carbide tools, thereby prolonging their service life. This can improve the performance of cutting tools and reduce downtime. The application of gas nitriding on different materials has a common goal, that is, to improve the hardness, wear resistance, and corrosion resistance of the material so as to increase the life and performance of the parts. However, the specific effects may vary depending on the type of material and the environment in which it is used. Therefore, when choosing gas nitriding as a surface treatment method, it is necessary to adjust the nitriding parameters and processes according to the specific application requirements.

The traditional method of gas nitriding has problems such as slow diffusion rate, high energy consumption, and uneven thickness of the infiltrated layer, which limits its application in industrial production [17][18]. The implementation of the “carbon peak, carbon neutral” strategy provides a strong driving force for the popularization and the application of nitriding wear-resistant and corrosion-resistant green surface treatment technology [19]. Improving the diffusion rate of gas nitriding is not only conducive to reducing energy consumption and achieving the goal of “carbon peak and carbon neutrality” but also can reduce production costs and expand the application field of nitriding technology. More and more scholars and researchers are conducting research on the new process of accelerating nitriding. Accelerating nitriding is a nitriding

method that uses the accelerating method to promote the diffusion of nitrogen atoms on the metal surface, which can significantly increase the diffusion rate of nitrogen atoms and reduce nitriding time and energy consumption. It can also achieve uniform layer thickness and reduce residual stress at the same time [20]. **Figure 1** shows the application of accelerating nitriding in the field of wind power. Among these processes, process parameter optimization [2][21][22], surface mechanical nano-crystallization [23][24][25], surface active catalysis [26][27][28], surface pre-oxidation [29][30][31], and surface laser treatment [32][33][34] are relatively common accelerating nitriding methods. The development of accelerating nitriding methods is also expected to expand its application in other fields. For example, nitriding technology has important application value in new energy materials [35][36], nano-materials [37][38], biomedicine [39][40], and other fields. Therefore, strengthening the research and development of accelerating nitriding methods will help to promote its application and promotion in industrial production and other fields.

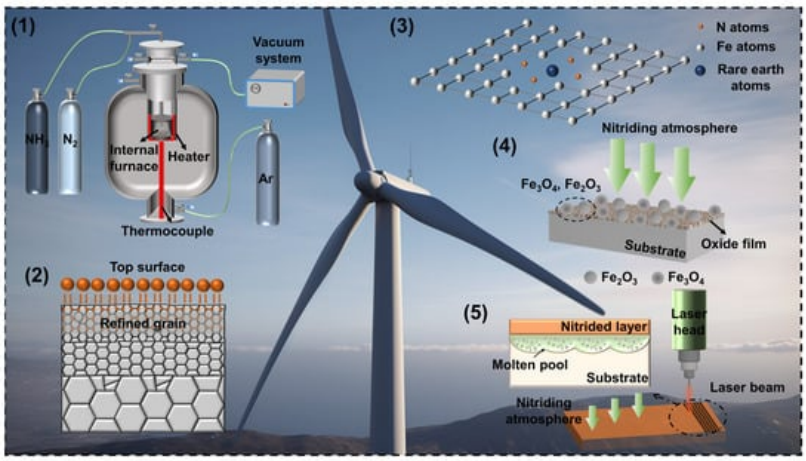

Figure 1. Application of accelerating gas nitriding in wind power field: (**1**) process parameter optimization, (**2**) Surface Mechanical Nano-Crystallization, (**3**) surface-active catalytic nitriding, (**4**) surface pre-oxidized nitriding, and (**5**) surface laser treatment.

2. Research Progress of Conventional Gas Nitriding

2.1. Mechanism of Gas Nitriding

Gas nitriding is a surface strengthening technology that makes the nitriding atmosphere penetrate to the surface of metal or alloy material and diffuse to a certain depth under the conditions of high temperature and high pressure [32][41]. During gas nitriding, nitrogen atoms chemically react with metal surface atoms to form a nitrided layer that is hard, wear resistant, corrosion resistant, and metal fatigue resistant. Gas nitriding generally uses NH_3, NH_3 + N_2, or NH_3 + H_2 as the gas medium [42]. **Figure 2** shows the gas nitriding interface reaction process [4]. The whole nitriding process is divided into three stages: decomposition of NH_3, adsorption of active N atoms ([N]), and diffusion of active N atoms ([N]) [3]. The ammonia gas entering the nitriding furnace cavity is divided into two parts: one part is directly thermally decomposed ammonia gas ($\mathrm{NH}_3^{\mathrm{D}}$), and the other part is undecomposed residual ammonia gas flowing through the surface of the workpiece in the form of NH_3 molecules ($\mathrm{NH}_3^{\mathrm{R}}$). Gas nitriding mainly depends on the interface reaction between the ammonia gas ($\mathrm{NH}_3^{\mathrm{R}}$) flowing through the surface of the workpiece . It can be seen from **Figure 2** that the effective infiltration of N atoms depends on the adsorption, decomposition, and absorption process of ammonia on the workpiece surface. The active N atoms generated by the thermal decomposition of $\mathrm{NH}_3^{\mathrm{R}}$ participate in the nitriding reaction and diffuse into the substrate to form a nitrided layer and promote it to grow thicker [5][44][45]. Therefore, according to **Figure 2**, the basic mechanism of gas nitriding is analyzed from the physicochemical reaction, adsorption, and diffusion of active N atoms ([N]).

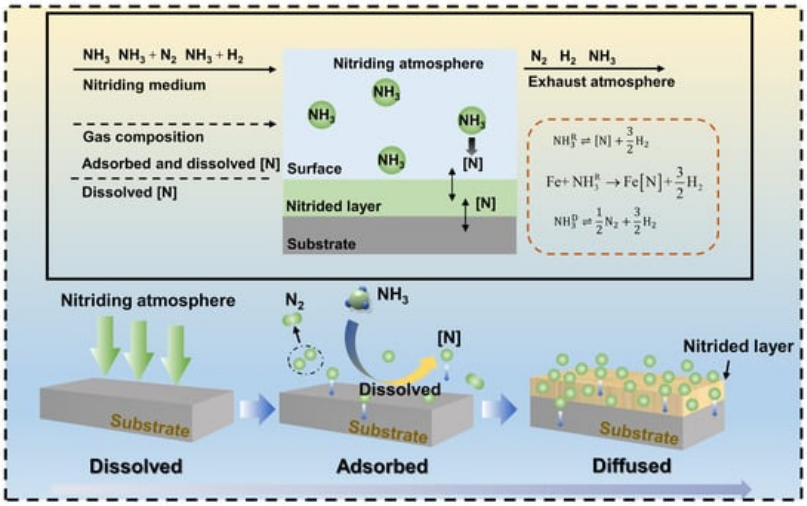

Figure 2. Interface reaction process of gas nitriding.

2.2. Nitrided Layer Structure of Gas Nitriding

Gas nitriding forms a surface layer with a high nitrogen concentration on the surface of metal by exposing metal samples to reactive gases such as nitrogen. This surface layer is called the nitrided layer [46].

The nitrided layer usually consists of two regions: the case-hardened layer and the hardened layer. The case-hardened layer is usually located on the surface of the nitrided layer and consists of a solid solution with a high nitrogen concentration. The hardened layer is located below the case-hardened layer and consists of solid solutions and nitrides with a relatively low nitrogen concentration. The hardened layer has higher toughness and strength, while the case-hardened layer has higher hardness [47].

During the nitriding process, the interaction of Fe and N can be analyzed through the phase diagram of the Fe-N binary alloy (as shown in **Figure 3**) [48]. The phase diagram includes two interstitial solid solutions, α and γ, and three interstitial phases, γ′, ε, and ζ. There are two eutectoid transitions in the phase diagram: at 592 °C and 2.4 wt.% N, the γ → α + γ′ eutectoid transition occurs; at 650 °C and 4.5 wt.%, ε → γ + γ′ eutectoid transformation occurs. The phase diagram of the Fe-N binary alloy shows that the mutual solubility of Fe and N is extremely low, and the solid solution can only be formed under high-temperature and high-pressure conditions. At room temperature, the nitrided layer is mainly composed of two phases: a nitride phase and a retained austenite phase. The nitride phase mainly includes Fe_4N, Fe_3N, and Fe_2N [49]. Among them, Fe_4N has the best thermal stability and is most commonly used in the nitriding process [50]. The retained austenite phase is mainly unnitrided austenite structure. The crystal structure of each phase is analyzed separately as follows:

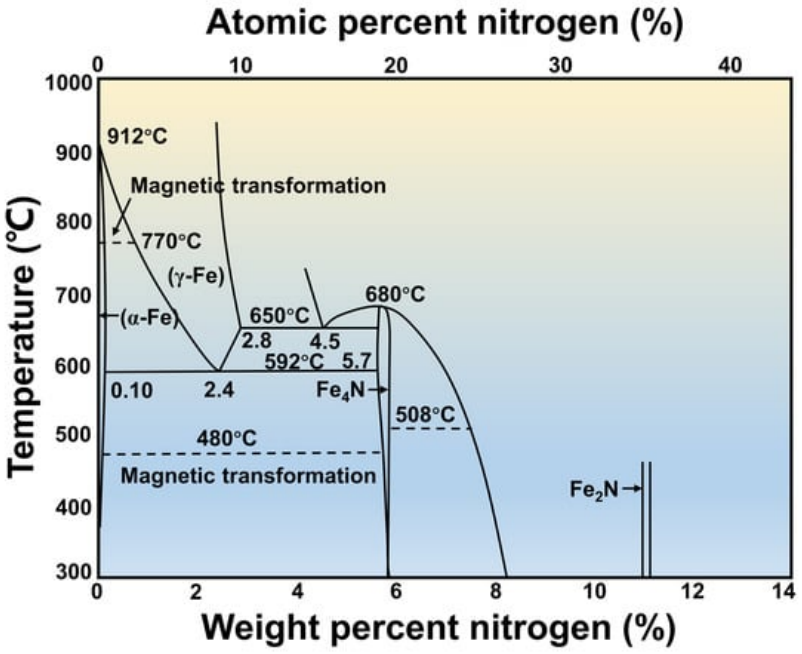

Figure 3. Phase diagram of Fe-N binary alloy.

The α phase belongs to the retained austenite phase of the nitrided layer. It is an interstitial solid solution of N in α-Fe, also known as nitrogen-containing ferrite. The lattice structure is a body-centered cubic structure and N atoms are located in the octahedral gap in the α-Fe lattice.

The γ phase belongs to the nitride phase in the nitrided layer. It is an interstitial solid solution of N in γ-Fe, also known as nitrogen-containing austenite. The lattice structure is a face-centered cubic structure, and N atoms are randomly distributed in the octahedral gaps in the γ-Fe lattice. The γ phase undergoes eutectoid reaction at 592 °C. Eutectoid decomposition occurs during slow cooling. γ → α + γ′ eutectoid decomposition occurs during slow cooling. During rapid cooling, γ → α′ transformation occurs, and the γ′ phase transforms into nitrogen-containing martensite (α′ phase) or exists in the state of retained austenite.

The γ′ phase, an interstitial phase with a nitrogen content between 5.7 wt.% and 6.1 wt.% and a variable composition, is represented by γ′-Fe_4N. γ′-Fe_4N has a stable structure, and N atoms orderly occupy the interstitial positions of the face-centered cubic lattice composed of Fe atoms. When the temperature is above 680 °C, it will decompose and transform into ε-$Fe_{2-3}N$.

The ε phase belongs to the nitride phase in the nitrided layer. It is a solid solution based on Fe_3N, represented by ε-$Fe_{2-3}N$. In the compound, N atoms orderly occupy the gaps of the close-packed hexagonal lattice composed of Fe atoms. The ε phase is a ferromagnetic phase, and the eutectoid decomposition of ε → γ + γ′ occurs at 650 °C.

The ζ phase belongs to the nitride phase in the nitrided layer. It is a kind of interstitial solid solution based on Fe_2N compound with an orthogonal rhombic lattice and nitrogen content between 11.07–11.18 wt.% and is brittle. The ζ phase transforms into the ε-$Fe_{2-3}N$ phase above 520 °C.

2.3. Process Parameters of Gas Nitriding

The process parameters that affect the efficiency of gas nitriding are mainly nitriding temperature, nitriding time, atmosphere pressure, and NH_3 flow rate. These parameters complement each other in the nitriding process.

(1) Nitriding temperature is an important parameter in the gas nitriding process, which will have a significant impact on the formation and the performance of the nitrided layer. Usually, the nitriding temperature is between 450 and 580 °C. If the temperature is too high, it will lead to excessive nitride formation, which will make the nitrided layer brittle. However, for stainless steel, although increasing the nitriding temperature can increase the thickness of the nitrided layer, it will also cause thermal decomposition of the γ_N-Fe phase and reduce the corrosion resistance of stainless steel, which is not advisable [51][52]. Studies have shown that the nitriding rate increases with the increasing temperature within a certain range. However, the depth of the nitrided layer shows a trend of increasing first and then decreasing, and there is an optimal temperature range. This is due to the fact that the growth of the nitrided layer is limited by solid-phase diffusion and liquid-phase diffusion [53].

(2) Nitriding time: Exposure time of metal samples in nitriding atmosphere. Typically, the nitriding time is between 2 and 48 h, depending on the type of material, size, and desired nitriding depth. Generally speaking, a longer nitriding time is conducive to the formation of a dense nitrided layer, which improves its hardness and wear resistance. However, too long a nitriding time will also lead to grain coarsening and surface roughness of the nitrided layer [54][55].

(3) Atmospheric pressure is also one of the important parameters affecting nitriding. Usually, the pressure during nitriding is between 0.1 and 2.0 MPa. As the atmosphere pressure increases, the nitriding rate and penetration depth gradually increase [56].

(4) Nitrogen flow: When gas nitriding, the flow rate of nitrogen is also an important parameter, it is usually between 5 L/min and 50 L/min [57].

(5) Nitriding media [58]: there are many types of nitriding media, and the common ones are as follows:

Ammonia: Ammonia is one of the most commonly used nitriding media in gas nitriding. It can realize high-speed nitriding at a lower temperature and form a uniform nitrided layer. Ammonia can also control the depth and the hardness of the nitrided layer by adjusting the temperature and ammonia flow. However, ammonia gas is toxic and flammable and requires special safety measures during nitriding.

Nitrogen: Nitrogen is an inert gas that can be used as a nitriding medium for nitriding. The rate of nitrogen nitriding is slow, requiring higher temperature and longer time to achieve a certain depth of nitrided layer. However, nitrogen has the

advantages of stability and safety and will not have adverse effects on the human body and the environment.

Mixed composition: Mixed gas refers to the nitriding medium that mixes different gases, such as ammonia and nitrogen, in a certain proportion. The mixed gas can combine the advantages of ammonia and nitrogen, can realize high-speed nitriding at lower temperature and time, and can control the depth and the hardness of the nitrided layer. However, the cost of mixed gas is relatively high.

3. Effect of Accelerating Nitriding Methods on the Behavior and Efficiency of Gas Nitriding

3.1. Process Parameter Optimization

3.1.1. Accelerating Nitriding Mechanism of Optimizing Process Parameters

Nitriding workpieces are required to have a hard and tough nitrided layer under actual service conditions, which mainly depends on the structure of the nitrided layer (γ′ phase and ε phase). The porous ε phase is the main cause of embrittlement and spalling of the nitrided layer. Therefore, controlling the composition of the white layer of the nitrided layer or making the white layer disappear is the focus of research [56][59].

Some scholars put forward the concept of controllable nitriding, which was called computer-controlled gas nitriding [60]. Based on Lehrer's point of view (**Figure 4**a), using the relationship between the limit nitrogen potential and temperature (Equation (1)) [18][61], a computer-controlled, fully industrially automated gas nitriding control system has been designed and applied successfully. Its commercial registration name is NITREG [62]. Michalski et al. [61] used controllable gas nitriding (NITREG®) to obtain a nitrided layer containing only γ′-Fe_4N-phase nitrides on the surface of carbon steel. Subsequently, the team used this method to prepare dense compound layers and nitrided layers without compound layers on the surface of 40HM and 38HMJ steels. Among them, the nitrided layers of 40HM and 38HMJ steels without compound layers showed the highest hardness values, respectively >700 $HV_{0.5}$ and 1100 $HV_{0.5}$ [21].

$$K_N = \frac{1-\omega}{(0.75\omega)^{1.5}} \quad (1)$$

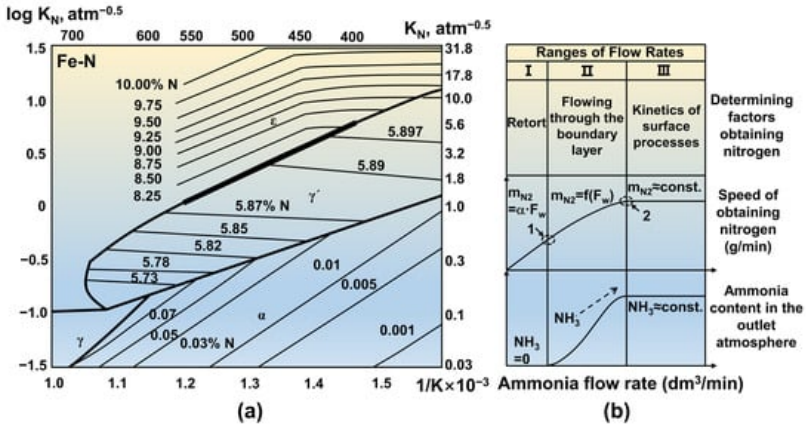

Figure 4. (**a**) Lehrer Fe−N equilibrium phase diagram and (**b**) the relationship between ammonia decomposition nitrogen production and ammonia content in the furnace atmosphere and the flow rate of ammonia gas flowing into the furnace.

Figure 4b shows the relationship between the nitrogen production rate of ammonia decomposition and the ammonia content in the furnace atmosphere and the ammonia gas flow into the furnace [63].

In the first stage, the flow rate of ammonia gas is very small. The rate of nitrogen production is proportional to the flow rate of ammonia gas entering the furnace, and the atmosphere out of the furnace only contains the decomposition products of ammonia. With the further increase in the ammonia gas flow rate to point 1, the contact time between the ammonia molecules and the workpiece surface is so short that some of the ammonia molecules cannot be decomposed. Therefore, the atmosphere of the furnace is nitrogen, hydrogen, and ammonia.

In the second stage, the nitrogen production rate is mainly determined by the ammonia content on the surface of workpiece. The rate of nitrogen production increases with the increase in the ammonia flow rate and tends to be stable at point 2.

When the flow of ammonia gas enters the third stage, the yield of nitrogen remains constant, and the amount of nitrogen produced is determined by the reaction kinetics (adsorption, desorption, and chemical adsorption) on the surface of the workpiece [57]. This shows that it is meaningless to study the nitrogen potential in stage III.

The nitrogen potential (K_N) is one of the factors to be considered in the study of the growth kinetics of the nitrided layer. As shown in Equations (2) and (3), the nitrogen potential is determined by temperature and pressure. Therefore, the effects of process parameters on gas nitriding and nitriding behavior are introduced from the two aspects of pressure and temperature.

$$K_N\gamma'/\varepsilon = \left[\exp\left(\frac{60536}{T} - 56.85\right)^{0.5} - 9.63\right] \times \left(1.013 \times 10^5\right)^{0.5} \quad (2)$$

$$K_N = \frac{P_{NH_3}}{(P_{H_2})^{1.5}} \quad (3)$$

3.1.2. Effect of Process Parameter Optimization on Nitriding Behavior

Effect of Pressure on Nitriding Behavior

Pressure is one of the factors affecting nitriding efficiency. From the ammonia decomposition formula, it can be seen that increasing the pressure can inhibit the decomposition of ammonia, reduce the decomposition rate of ammonia, and increase the nitrogen potential [56]. Fu et al. [49] developed a special pressurized gas equipment—a new type of gas nitriding furnace with a dual-pressure balance structure. The schematic diagram of the equipment is shown in **Figure 5**a. NH_3 and Ar at the same pressure are fed into the inner furnace and outer furnace, respectively, and the pressure in the reaction chamber can be adjusted in a wide range by balancing the pressure of the inner and outer layers of the inner furnace wall to realize high-pressure gas nitriding. The equipment can ensure the smooth progress of the gas nitriding within the pressure range of 0–1.0 MPa.

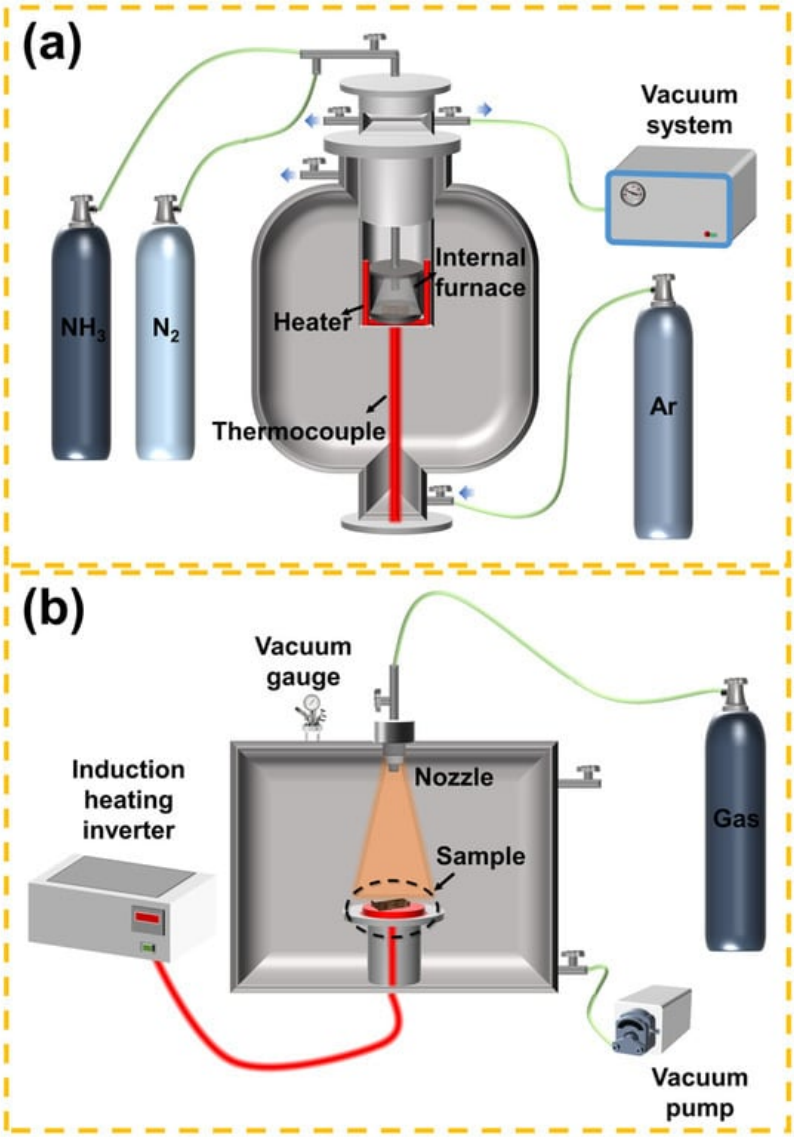

Figure 5. (**a**) Simplified diagram of pressurized gas nitriding equipment. (**b**) Schematic diagram of gas-blown induction heating (GBIH) nitriding plant.

Shogo et al. [64] used a nitriding device to characterize the surface modification layer of Ti-6Al-4V alloy produced by gas-blown induction heating (GBIH). The schematic diagram of the device is shown in **Figure 5**b. The device studies the effect of temperature on nitriding behavior by monitoring the internal temperature of the material, the electrical effect generated by induction heating (IH), nitrogen gas blowing, and the effect of passivation film on titanium alloys. It was found that the nitrided layer obtained by GBIH nitriding was thicker than that calculated from the diffusion coefficient inside the sample at high temperature. This is because during the nitriding process of GBIH, the electric effect generated by IH makes part of the nitrided layer to form rapidly. The electric effect of IH can also make the passivation film on the surface of Ti-6Al-4V alloy disappear rapidly during the GBIH nitriding process. Since the GBIH nitriding treatment is carried out under the condition of controlled atmosphere, the passivation film on the surface of the alloy will not be regenerated. Only a few minutes of GBIH nitriding can form nitrided layers on the surface of Ti-6Al-4V alloy, and the characteristics of these nitrided layers are similar to those formed after several hours of ordinary gas nitriding [65][66][67]. GBIH nitriding can modify Ti-6Al-4V alloy in a short time, mainly due to the electrical effect and the disappearance of passivation film produced by nitriding.

3.1.3. Effect of Process Parameter Optimization on Nitriding Efficiency

The influence of process parameter optimization on nitriding efficiency was compared and analyzed from the four aspects of nitriding time, nitriding temperature, nitriding layer structure, and nitriding layer hardness. According to the literature summary, and after taking the average value, the comparison histogram of parameter optimization gas nitriding and conventional gas nitriding efficiency uniformity is obtained, as shown in **Figure 6**.

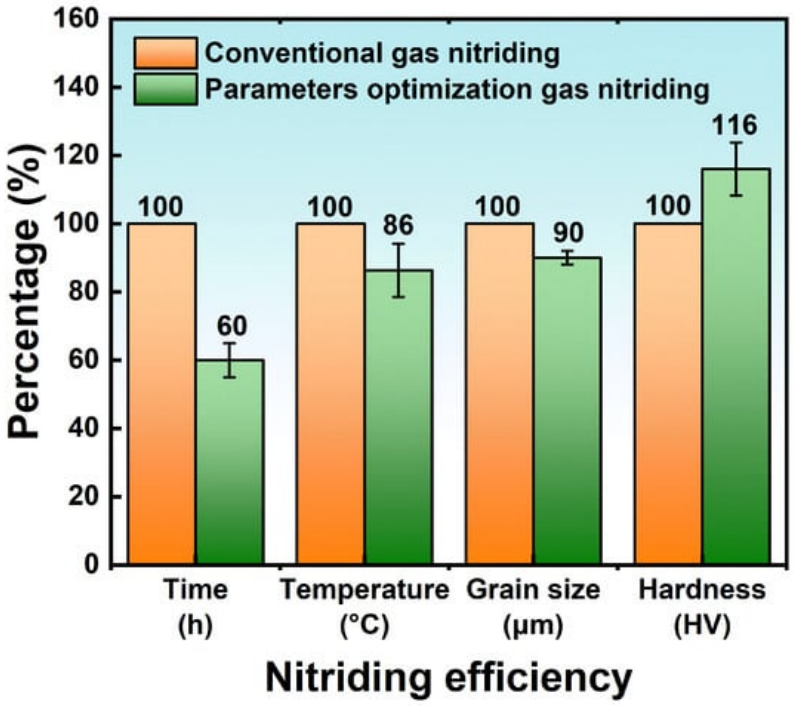

Figure 6. Histogram of efficiency comparison between parameter-optimized gas nitriding and conventional gas nitriding.

3.2. Surface Mechanical Nano-Crystallization

3.2.1. Accelerating the Nitriding Mechanism of Surface Mechanical Nano-Crystallization

Surface mechanical nano-crystallization (SMAT) is a method of using mechanical impact to cause strong plastic deformation on the surface of the material at a high strain rate, thereby forming nano-scale grains on the surface while there is no impurity pollution inside the metal material [68]. Generally, mechanical processing or heat treatment methods, such as shot blasting and surface mechanical abrasion treatment, are used to realize surface self-nano-crystallization on the metal surface, and to obtain the gradient nano-structure surface layer whose grain size gradually increases along the thickness direction [69].

Although the preparation methods of surface deformation nano-scale are different, the mechanism of surface grain refinement and strengthening is basically the same. Both use specific mechanical methods to increase the free energy of the metal material surface, so that the surface of the material undergoes strong plastic deformation at a high strain rate, thereby forming sub-grain boundaries, small-angle grain boundaries, dislocations, and twins within the grains. And, there is an interaction between them to divide the large grains on the metal surface to refine the grains, thereby realizing the nano-crystallization of the surface layer [70]. Based on the observation of the microstructure, it is found that when the metal material is deformed to produce grain refinement, the following process generally occurs: (1) formation of high-density dislocation walls (DDWs) and dislocation tangles (DTs) in the original grains; (2) high-density dislocation wall and transformation of dislocation entanglements into single crystals or sub-grains separated by low-angle grain boundaries; (3) sub-grain boundary evolves into high-angle grain boundary [71][72]. The mechanism of grain refinement is shown in **Figure 7**.

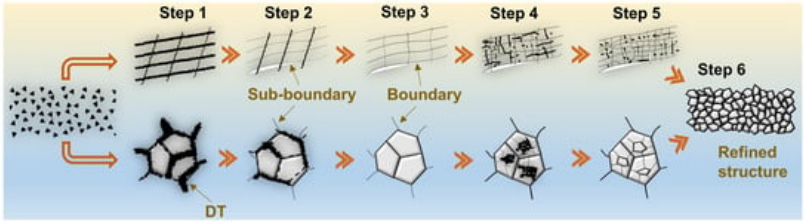

Figure 7. Grain refinement mechanism diagram of surface mechanical nano-crystallization.

3.2.2. Effect of Surface Mechanical Nano-Crystallization on Nitriding Behavior

The formation of the nitrided layer in the gas nitriding process begins at certain energy-rich places, such as grain boundaries, surface defects and impurities, etc. [73]. Unlike the substrate nitriding, the metal surface nano-layer has a high density of grain boundaries, such as dislocations, twins, and sub-grain boundaries, which provide ideal diffusion channels for N atoms [74]. The density of the lattice defects is also one of the conditions affecting the thickness of the nitrided layer.

The nano-sized surface increases the grain boundary defects, provides an ideal channel for the diffusion of N atoms, significantly reduces the activation energy of N atom diffusion, and improves the nitriding kinetics [75].

SMAT nitrided specimens have a thicker compound layer, a unique transition zone, and a diffuse layer with a small amount of acicular nitride. This excellent nitrided layer structure makes the SMAT nitrided samples show more excellent hardness and wear resistance [3][75]. Subsequent studies have also found that SMAT can also increase the thickness of the steel layer and accelerate the rate of nitride formation [76][77]. And, for the Cr-containing steel, a small amount of Fe_4N phase was formed in the SMAT nitrided sample, which was due to the high-temperature-induced nitride nucleation.

Balusamy et al. [78] found that the increase in martensite content and the decrease in surface roughness are conducive to the diffusion of nitrogen atoms, promote the precipitation of the element Cr, and form a higher content of CrN. Moreover, a passivation layer with a thickness of 60–120 nm is formed. The formation of this type of passivation layer will inevitably have a great impact on the corrosion resistance of the sample. Lin [79] and Zhang [80] found that compared with untreated nitriding samples, the wear life of SMAT-treated nitriding samples was 3 to 10 times that of untreated samples. This is because SMAT pretreatment promotes the formation of a nitrided layer and a gradient diffusion layer, which makes SMAT nitrided samples have higher hardness and bearing capacity.

In summary, the surface mechanical nano-technology can effectively promote the nitriding process on the surface of metal materials, reduce the nitriding temperature, increase the thickness of the nitriding layer, reduce the nitride crystal size, increase the nitride content, and improve the composite modified layer's performance.

3.2.3. Effect of Surface Mechanical Nano-Crystallization on Nitriding Efficiency

The effects of surface mechanical nano-crystallization on nitriding efficiency are compared and analyzed from the four aspects of nitriding time, nitriding temperature, structure of the nitrided layer, and hardness of the nitrided layer. According to the summary of the literature, the comparison histogram of the uniformity of surface nano-gas nitriding and conventional gas nitriding efficiency is obtained after taking the average values, as shown in **Figure 8**.

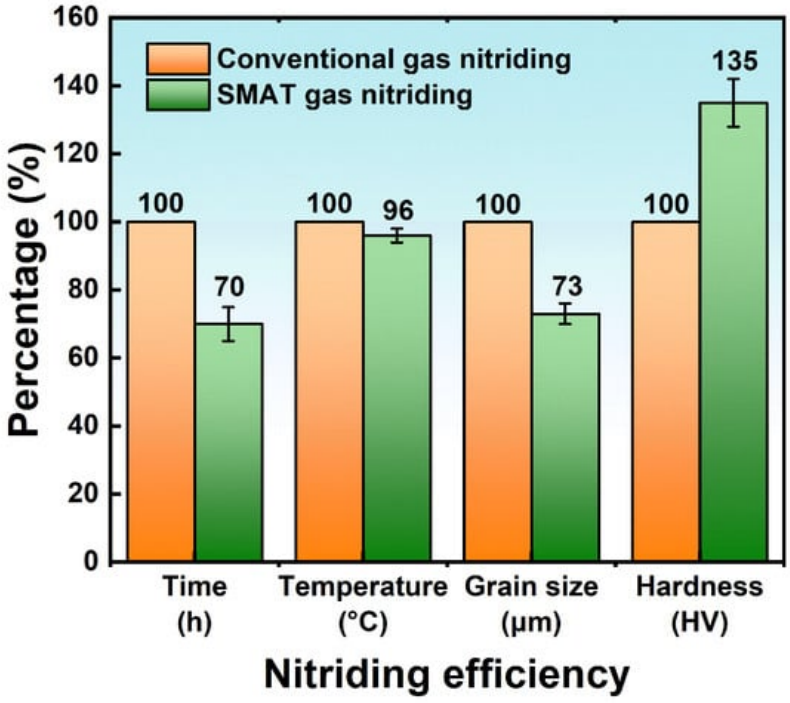

Figure 8. Histogram of efficiency comparison between surface mechanical nano-crystallization gas nitriding and conventional gas nitriding.

3.3. Surface-Active Catalytic Nitriding

3.3.1. Accelerating Nitriding Mechanism of Surface-Active Catalytic Nitriding

Surface-active catalytic nitriding is a technology that uses surface catalysts to promote gas reactions on the surface of materials. Adding a surface-active infiltrating agent into the furnace by means of surface coating, dripping, and gas-solid mixing can reduce the activation energy of the workpiece surface during gas nitriding. It can also increase the decomposition rate of adsorbed ammonia on the workpiece surface, realize low-temperature gas nitriding, and improve nitriding efficiency [26][27]. During the gas nitriding process, surface-active catalysis nitriding can provide additional reaction

sites and promote the adsorption and reaction of nitrogen molecules to accelerate the nitriding rate [81]. In addition, surface-active catalytic nitriding can realize the nitriding reaction at a lower temperature and reduce the influence of nitriding temperature on the material to improve the heat resistance and mechanical properties of the material [82]. Overall, surface-active catalysis is an effective gas nitriding technology that can achieve an efficient nitriding process at lower temperatures, resulting in improved material performance and durability.

3.3.2. Effect of Surface-Active Catalytic on Nitriding Behavior

Effect of Alloying Elements (Ni, C, Ti, B, etc.) on Nitriding Behavior

During the gas nitriding process, the nitrogen atoms absorbed on the surface of the workpiece participate in the nitriding reaction and diffuse into the matrix, resulting in the development of the diffusion zone. In the nitrogen supply medium (nitriding atmosphere), iron can directly react with nitrogen, resulting in the formation of a layer of iron nitride on the surface of the sample at the top of the diffusion zone when the nitrogen potential is high enough. This layer of iron nitride is the so-called compound layer [83]. The active catalysis of alloying elements uses its affinity for nitrogen more strongly than for iron and preferentially interacts with nitrogen in the diffusion zone to regulate the phase characteristics of the nitrided layer and improve the performance of the nitrided layer [84]. The grain composition, crystal structure, and morphology of alloying elements (Me) and nitrides (MeN_x) have a significant effect on controlling the properties of iron-nitride-based components [85].

The precipitation kinetics of nitrides are mainly affected by the development of misfit-strain fields and their relaxation rates caused by the coherent→incoherent transition at the Me-nitride/α-Fe interface [86][87]. It is now possible to precisely determine the various types of (excess) nitrogen present in the nitrided microstructure. Armed with this knowledge, physics-based models are being developed that can describe nitriding behavior.

Steiner et al. [85] found that carbides were less stable than nitrides by comparing the Gibbs formation energies of carbides and nitrides. At 773 K (500 °C), the Gibbs formation energy of Ti to TiN is -268 kJ/mol, and the Gibbs formation energy of Ti to TiC is -174 kJ/mol. During the nitriding process, the carbides generated due to the tempering treatment are dissolved, reprecipitated, or directly converted into nitrides. If a compound layer is formed on the surface of the sample, the carbon released by the nitride formation may infiltrate into the compound layer if the nitrogen potential in the surrounding atmosphere is sufficiently high. If the compound layer cannot be formed on the surface of the sample, the carbon will diffuse into the atmosphere. Especially at a greater depth from the surface of the compound layer, the carbon released by the formation of nitrides may lead to local supersaturation of carbon so that carbon is precipitated in the form of cementite Fe_3C. During the nitriding process, the macroscopic compressive stress parallel to the surface of the compound layer along the diffusion zone makes the cementite preferentially formed on the grain boundary.

3.3.3. Effect of Surface-Active Catalytic Nitriding on Nitriding Efficiency

The effects of surface-active catalytic nitriding on nitriding efficiency are compared and analyzed from the four aspects of the nitriding time, nitriding temperature, structure of nitrided layer, and hardness of nitrided layer. As shown in **Figure 9**, the efficiency comparison histogram of surface-active catalytic nitriding and conventional gas nitriding is obtained after taking the average value according to the literature summary.

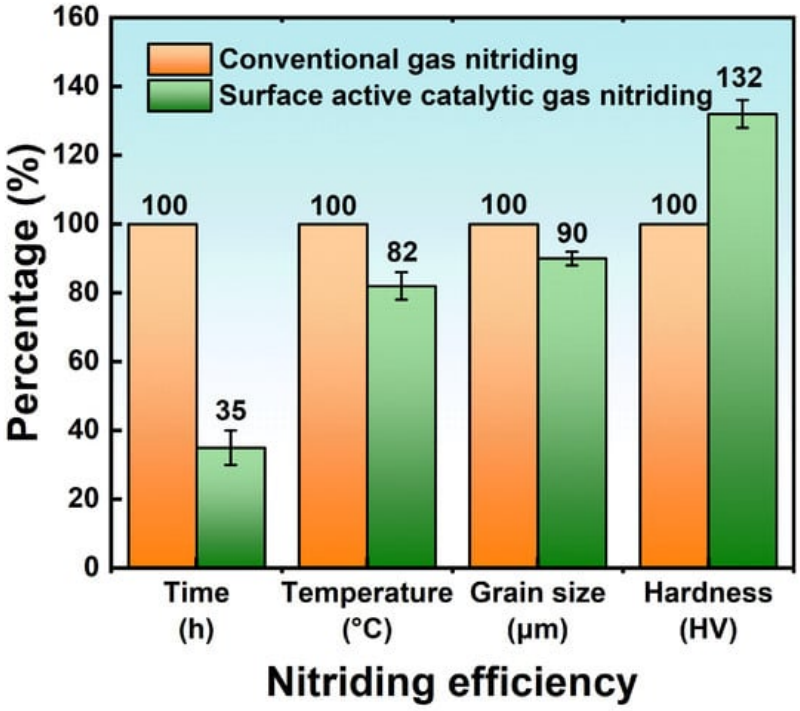

Figure 9. Histogram of efficiency comparison between surface-active catalytic nitriding and conventional gas nitriding.

3.4. Surface Pre-Oxidized Nitriding

3.4.1. Accelerating Nitriding Mechanism of Surface Pre-Oxidized Nitriding

When the metal surface is treated by the method of pre-oxidation, a thin oxide film will be formed on the metal surface, and this oxide film is mainly composed of Fe_3O_4 and Fe_2O_3. surface pre-oxidation will form a thin layer of dense oxide film on the surface of the workpiece, during which the following reactions occur [88]:

$$4Fe + 3O_2 = 2Fe_2O_3,\ 3Fe + 2O_2 = Fe_3O_4 \quad (4)$$

$$3Fe + 4H_2O = Fe_3O_4 + 4H_2 \quad (5)$$

In the gas nitriding stage, under the reducing action of ammonia and hydrogen, the oxide film is continuously reduced and combined with active nitrogen atoms, enriched on the surface of the workpiece. And, because the oxide film is continuously reduced to form a loose and porous structure, the diffusion channel of nitrogen atoms is increased, and the chance of nitrogen atoms being adsorbed on the surface is increased [30]. The following reactions may occur:

$$4Fe_3O_4 + 4NH_3 = 4Fe_3N + 6H_2O + 5O_2 \quad (6)$$

$$[Fe] + x[N] \rightarrow Fe_xN \quad (7)$$

$$4H_2 + Fe_3O_4 = 3Fe + 4H_2O \quad (8)$$

It can be seen from Equations (4)–(8) that the oxide film is constantly replaced by nitride to increase the thickness of the effective nitrided layer and improve the nitriding efficiency.

There are three main methods of surface pre-oxidation: air pre-oxidation, anodic oxidation, and micro-arc oxidation technology [89][90].

The air pre-oxidation method places the workpiece in the air and heats it to 300–600 °C (usually 450–500 °C is the best), and the holding time is 30–90 min to oxidize the surface to form a thin oxide film. The air pre-oxidation method has the advantages of simple operation, low cost, and no need to add additional equipment, so it is suitable for promotion in industrial production [91].

The anodic oxidation method is the process of preparing an oxide film on the surface of the anode in the corresponding electrolyte under the action of an external current using electrode reaction and electric field drive to make metal particles and oxygen ions migrate directionally.

3.4.2. Effect of Surface Pre-Oxidation on Nitriding Behavior

Surface pre-oxidation can increase the diffusion rate of nitrogen atoms and promote the formation of nitrides. It can also improve the initial wear resistance, seizure resistance, and mechanical fatigue strength of the workpiece surface. After adopting the surface pre-oxidized nitriding, Zhang et al. [92] found that the thickness of the nitrided layer on the surface of the base material 42CrMo steel increased, and the thickness of the effective diffusion layer was significantly improved.

Under the same nitriding process, the thickness of the nitrided layer without surface pre-oxidation treatment is only 6.15 μm. However, the thickness of the nitrided layer after surface pre-oxidation treatment increased. And, when the pre-oxidation process is 300 °C × 30 min, the thickness of the nitrided layer reaches the maximum value of 15 μm. Li et al. [30] [93] used the Owens–Wendt formula to calculate the surface free energy of 42CrMo steel treated with different pre-oxidation processes. The surface free energy calculation formula is as follows:

$$\gamma s=\gamma ps+\gamma ds \quad (6)$$

where γ_s is the surface free energy, γps is the polar component of the surface free energy, and γds is the dispersive component of the surface free energy. The results show that when the pre-oxidation process is 300 °C × 30 min, the γps and γds are the largest. The surface free energy calculated by Formula (14) is the largest. The higher the surface free energy is, the more unstable the structure is, thus playing a significant role in promoting gas nitriding [89].

In summary, the surface pre-oxidation treatment process has a significant catalytic effect on nitriding. The compound layer on the surface of the workpiece after surface pre-oxidation treatment is thicker than that of the conventional nitriding workpiece, and the thickness of the effective diffusion layer is significantly increased. After surface pre-oxidation, a large number of uniformly distributed nano-scale oxide particles are formed on the surface of the material, accompanied by microcracks and holes. And the surface free energy is the largest. These surface features are conducive to the adsorption of nitrogen and further diffusion to the substrate, thereby effectively increasing the nitriding rate. The microstructure of the nitrided layer on the surface of the surface pre-oxidized sample is mainly composed of ε-Fe_3N and γ′-Fe_4N phases. The white, light layer part is mainly ε phase, and the gray layer part is γ′ phase [37][61]. As the thickness of the nitrided layer increases after pre-oxidation, the friction coefficient of the sample surface tends to decrease, and the surface pre-oxidation improves the initial wear resistance of the sample surface.

3.4.3. Effect of Surface Pre-Oxidation on Nitriding Efficiency

The effects of surface pre-oxidation on nitriding efficiency are compared and analyzed from the four aspects of the nitriding time, nitriding temperature, structure of the nitrided layer, and hardness of the nitrided layer. As shown in **Figure 10**, the efficiency comparison histogram of surface pre-oxidized nitriding and conventional gas nitriding is obtained after taking the average value according to the literature summary.

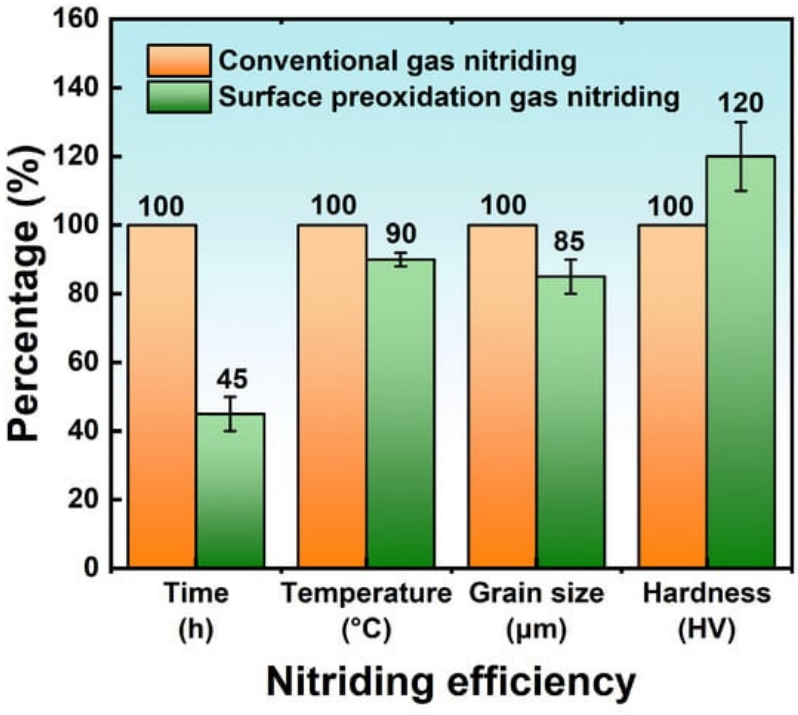

Figure 10. Histogram of efficiency comparison between surface pre-oxidized nitriding and conventional gas nitriding.

3.5. Surface Laser Treatment

3.5.1. Accelerating Nitriding Mechanism of Surface Laser Treatment

Figure 11 shows the mechanism of surface laser treatment catalytic nitriding. Surface laser treatment concentrates the energy of the laser beam on the surface of the material to increase the temperature and cool it rapidly to form a certain depth of melting zone and heat-affected zone, thereby improving the surface properties of the material, such as wear resistance, corrosion resistance, and mechanical fatigue life [32]. In the process of surface laser treatment, the selection of parameters such as laser beam power, scanning speed, and scanning line distance can affect the depth and shape of the nitrided layer, thereby controlling the properties of the treated material. The main mechanism includes the following aspects [32][33][34]:

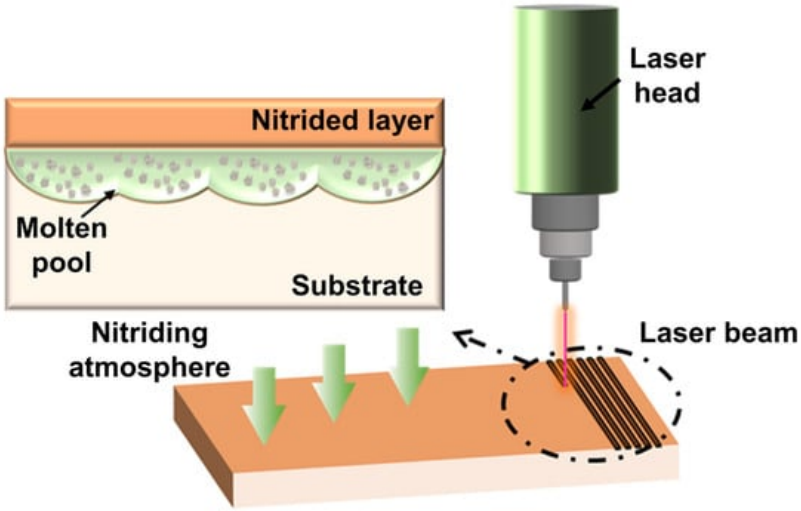

Figure 11. Schematic diagram of the mechanism of surface laser treatment catalytic nitriding.

3.5.2. Effect of Surface Laser Treatment on Nitriding Behavior

Surface laser treatment has been widely used in surface modification of materials and preparation of penetrants. In terms of gas nitriding, surface laser treatment also significantly affects nitriding behavior, which is mainly reflected in the following three aspects [32][68]: (1) Adjustment of the surface microstructure of the material and improvement of the surface reactivity and surface energy, thereby promoting the nitriding reaction; (2) changing the composition and chemical state of the penetrant, thereby changing the stoichiometry of nitride formation; and (3) controlling nitride deposition location and morphology by adjusting surface structure and energy distribution.

3.5.3. Effect of Surface Laser Treatment on Nitriding Efficiency

The effects of surface laser treatment on nitriding efficiency are compared and analyzed from the four aspects of the nitriding time, nitriding temperature, nitrided layer structure, and nitrided layer hardness. As shown in **Figure 12**, the efficiency comparison histogram of surface laser treatment catalytic nitriding and conventional gas nitriding is obtained after taking the average value according to the literature summary.

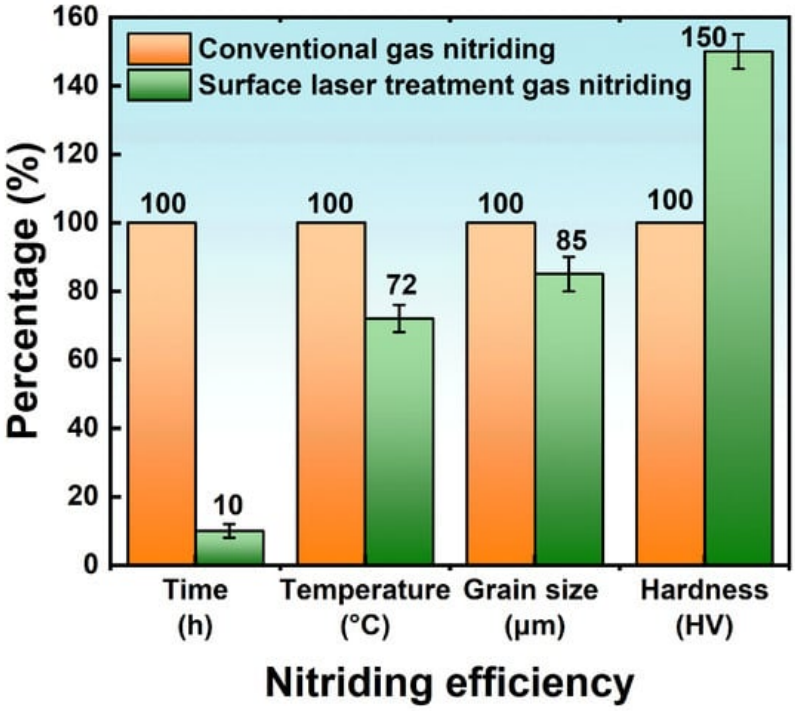

Figure 12. Histogram of efficiency comparison between surface laser treatment catalytic nitriding and conventional gas nitriding.

4. Conclusions

Optimizing process parameters is one of the most commonly used methods in gas nitriding. By adjusting the pressure and temperature of gas nitriding, the nitriding depth and nitriding rate can be controlled. However, optimizing process parameters requires precise control of temperature and pressure and may result in surface oxidation or chemical reactions that reduce the efficiency.

Surface mechanical nano-crystallization is another common accelerating method, which can improve the efficiency of gas nitriding by reducing the surface roughness. This method can increase the nitriding depth and nitriding rate without changing the chemical composition of the sample but requires the use of complex nano-fabrication techniques and may affect the mechanical properties of the sample.

Surface-active catalytic nitriding is a method of accelerating gas nitriding using surface-active penetrants. By coating the surface of the part with a penetrant, the nitriding temperature can be lowered and the nitriding rate and depth can be increased. However, penetrants may cause surface chemical reactions or degrade the mechanical properties of the part.

Surface pre-oxidation is a method of surface oxidation treatment before gas nitriding. It reduces the occurrence of surface chemical reactions and increases the efficiency of gas permeation. However, surface pre-oxidation requires the use of special oxidation treatments and may lead to peeling or destruction of the oxide layer.

Surface laser treatment changes the chemical and physical properties of the surface by laser irradiation, thereby improving the efficiency of gas penetration. This method can increase the nitriding depth and rate without changing the chemical composition of the sample but requires the use of high-power lasers and may affect the mechanical properties of the sample.

In addition, these methods also have different defects in terms of energy consumption, carbon dioxide emissions, and technical maturity. In terms of energy consumption, the gas nitriding process requires a large amount of energy. For example, gas nitriding under the conditions of high temperature and high pressure requires a lot of electricity or fuel. Therefore, it is necessary to explore gas nitriding penetrants and catalytic methods with low energy consumption. In terms of CO_2 emissions, high energy consumption means high CO_2 emissions. Therefore, it is necessary to develop a gas nitriding method with low energy consumption and low carbon dioxide emission to reduce the impact on the environment. In terms of technology readiness level, different methods have different degrees. For example, optimizing process parameters is one of the most commonly used gas nitriding methods, and the technology readiness level is relatively high. However, methods such as surface mechanical nano-crystallization and surface laser treatment are relatively new and require more experimental verification and optimization. Therefore, it is necessary to comprehensively consider factors

such as energy consumption, carbon dioxide emissions, and technology readiness level when selecting a gas nitriding and accelerating method and to strive to develop a more environmentally friendly, low-energy gas nitriding method.

Aiming at these problems, it may be a good solution to use multiple techniques for collaborative preprocessing. By combining different pretreatment methods, their advantages can be maximized, thereby improving the efficiency and environmental protection of gas nitriding. This also needs to be formulated according to the specific situation to ensure the maximization of comprehensive benefits. For example, the method of synergistic pretreatment of surface mechanical nano-crystallization and surface-active catalytic nitriding can be considered. Surface mechanical nano-crystallization can improve the surface quality and micro-morphology through micro-grinding or impact treatment, thereby improving the efficiency of gas nitriding. Surface-active catalytic nitriding can increase the reaction rate by introducing a penetrant on the surface or adding a penetrant during the gas nitriding process, thereby further improving the efficiency of gas nitriding. This method can simultaneously solve the problems of surface quality and reaction rate, thereby improving the comprehensive benefits of gas nitriding. In addition, the method of synergistic pretreatment of surface mechanical nano-crystallization and surface pre-oxidation can also be considered. Surface pre-oxidized nitriding can improve the quality and thickness of the surface oxide layer through oxidation treatment, thereby increasing the reaction sites of gas nitriding and increasing the reaction rate. This method can solve the problem of surface quality and reaction sites to improve the efficiency of gas nitriding. It should be noted that for different materials and application scenarios, different preprocessing methods may produce different effects. When selecting and combining pretreatment methods, it is necessary to consider the characteristics of the material and the specific application requirements to develop the best solution.

In summary, different gas nitriding methods have their advantages and disadvantages. Choosing an appropriate method requires comprehensive consideration of component materials, surface topography, and nitriding depth. Using the synergistic effect of multiple pretreatment methods can improve the efficiency and reliability of gas nitriding. It is of great value and significance for industry development, double carbon implementation, and green and sustainable development. It is one of the important directions for the development of gas nitriding technology in the future.

References

1. Michalski, J.; Wach, P.; Tacikowski, J.; Betiuk, M.; Burdynski, K.; Kowalski, S.; Nakonieczny, A. Contemporary industrial application of nitriding and its modifications. Mater. Manuf. Process. 2009, 24, 855–858.
2. Almeida, E.A.S.; Costa, C.E.; Milan, J.C.G. Study of the nitrided layer obtained by different nitriding methods. Matéria 2015, 20, 460–465.
3. Tong, W.P.; Liu, C.Z.; Wang, W.; Tao, N.R.; Wang, Z.B.; Zuo, L.; He, J.C. Gaseous nitriding of iron with a nanostructured surface layer. Scr. Mater. 2007, 57, 533–536.
4. Wang, B.; Fu, W.T.; Dong, F.; Jin, G.F.; Feng, W.W.; Wang, Z.H.; Sun, S.H. Significant acceleration of nitriding kinetics in pure iron by pressurized gas treatment. Mater. Des. 2015, 85, 91–96.
5. Keddam, M.; Djeghlal, M.E.; Barrallier, L. A diffusion model for simulation of bilayer growth (ε/γ′) of nitrided pure iron. Mater. Sci. Eng. 2004, 378, 475–478.
6. Alekseeva, M.S.; Gress, M.A.; Scherbakov, S.P.; Gerasimov, S.A.; Kuksenova, L.I. The influence of high-pressure gas nitriding on the properties of martensitic steels. Met. Sci. Heat Treat. 2017, 59, 524–528.
7. Singh, S.K.; Naveen, C.; Sai, Y.V.; Satish, U.; Bandhavi, C.; Subbiah, R. Experimental study on wear resistance of AISI 347 treated with salt bath nitriding and gas nitriding processes-a review. Mater. Today Proc. 2019, 18, 2717–2722.
8. Kim, Y.H.; Kim, H.G. Effect of Gas Nitriding Characteristics on the Mechanical Properties after Pre-Heat Treatment of Stainless Steels. J. Korean Soc. Heat Treat. 2010, 23, 142–149.
9. Boztepe, E.; Alves, A.C.; Ariza, E.; Rocha, L.A.; Cansever, N.; Toptan, F. A comparative investigation of the corrosion and tribocorrosion behaviour of nitrocarburized, gas nitrided, fluidized-bed nitrided, and plasma nitrided plastic mould steel. Surf. Coat. Technol. 2018, 334, 116–123.
10. Ichii, K. Structure of the ion-nitrided layer of 18-8 stainless steel. Technol. Rep. Kansai Univ. 1986, 27, 135.
11. Kundalkar, D.; Mavalankar, M.; Tewari, A. Effect of gas nitriding on the thermal fatigue behavior of martensitic chromium hot-work tool steel. Mater. Sci. Eng. 2016, 651, 391–398.
12. Pellizzari, M.; Molinari, A.; Straffelini, G. Thermal fatigue resistance of gas and plasma nitrided 41CrAlMo7 steel. Mater. Sci. Eng. 2003, 352, 186–194.

13. Akhtar, S.S.; Arif, A.F.M.; Yilbas, B.S. Evaluation of gas nitriding process with in-process variation of nitriding potential for AISI H13 tool steel. Int. J. Adv. Manuf. Technol. 2010, 47, 687–698.
14. Moradshahi, M.; Tavakoli, T.; Amiri, S.; Shayeganmehr, S. Plasma nitriding of Al alloys by DC glow discharge. Surf. Coat. Technol. 2006, 201, 567–574.
15. Funch, C.V.; Christiansen, T.L.; Somers, M.A.J. Gaseous nitriding of additively manufactured maraging steel; nitriding kinetics and microstructure evolution. Surf. Coat. Technol. 2022, 432, 128055.
16. Li, G.M.; Liang, Y.L.; Sun, H.; Cao, Y.G. Nitriding behavior and mechanical properties of carburizing and nitriding duplex treated M50NiL steel. Surf. Coat. Technol. 2020, 384, 125315.
17. Baranowska, J.; Arnold, B. Corrosion resistance of nitrided layers on austenitic steel. Surf. Coat. Technol. 2006, 200, 6623–6628.
18. Somers, M.A.J.; Mittemeijer, E.J. Layer-growth kinetics on gaseous nitriding of pure iron: Evaluation of diffusion coefficients for nitrogen in iron nitrides. Metall. Mater. Trans. A 1995, 26, 57–74.
19. Yang, S.; Yang, D.; Shi, W.; Deng, C.; Chen, C.; Feng, S. Global evaluation of carbon neutrality and peak carbon dioxide emissions: Current challenges and future outlook. Environ. Sci. Pollut. Res. 2023, 30, 81725–81744.
20. Karakan, M.; Alsaran, A.; Celik, A. Effect of process time on structural and tribological properties of ferritic plasma nitrocarburized AISI 4140 steel. Mater. Des. 2004, 25, 349–353.
21. Michalski, J.; Tacikowski, J.; Wach, P.; Ratajski, J. Controlled gas nitriding of 40HM and 38HMJ steel grades with the formation of nitrided cases with and without the surface compound layer, composed of iron nitrides. Probl. Eksploat. 2006, 2, 43–52.
22. Fattah, M.; Mahboubi, F. Comparison of ferritic and austenitic plasma nitriding and nitrocarburizing behavior of AISI 4140 low alloy steel. Mater. Des. 2010, 31, 3915–3921.
23. Kumar, S.A.; Raman, S.G.S.; Narayanan, T.S.N.S.; Gnanamoorthy, R. Influence of counterbody material on fretting wear behaviour of surface mechanical attrition treated Ti–6Al–4V. Tribol. Int. 2013, 57, 107–114.
24. Liu, B.; Wang, B.; Yang, X.D.; Zhao, X.F.; Qin, M.; Gu, J.F. Thermal fatigue evaluation of AISI H13 steels surface modified by gas nitriding with pre-and post-shot peening. Appl. Surf. Sci. 2019, 483, 45–51.
25. Liu, J.; Suslov, S.; Vellore, A.; Ren, Z.C.; Amanov, A.; Pyun, Y.S.; Martini, A.; Dong, Y.L.; Ye, C. Surface nanocrystallization by ultrasonic nano-crystal surface modification and its effect on gas nitriding of Ti6Al4V alloy. Mater. Sci. Eng. 2018, 736, 335–343.
26. Rodrigues, J.; Miranda, S.M.C.; Santos, N.F.; Neves, A.J.; Alves, E.; Lorenz, K.; Monteiro, T. Rare earth co-doping nitride layers for visible light. Mater. Chem. Phys. 2012, 134, 716–720.
27. Zhang, C.; Wang, Y.; Chen, X.; Chen, H.T.; Wu, Y.Q.; Wang, Y.X.; Tang, L.N.; Cui, G.D.; Chen, D.Z. Catalytic behavior of LaFeO3 pervoskite oxide during low-pressure gas nitriding. Appl. Surf. Sci. 2020, 506, 145045.
28. Zhang, C.S.; Yan, M.F.; Sun, Z. Experimental and theoretical study on interaction between lanthanum and nitrogen during plasma rare earth nitriding. Appl. Surf. Sci. 2013, 287, 381–388.
29. Sueyoshi, H.; Hamaishi, K.; Kadomatsu, S.; Shiomizu, T.; Ohzono, Y. Effect of preheating in air on gas nitriding of SUS304. Nippon Kinzoku Gakkaishi (1952) 1996, 60, 616–623.
30. Lutz, J.; Mändl, S. Effect of ion energy and chemistry on layer growth processes during nitriding of CoCr alloys. Nucl. Instrum. Methods Phys. Res. Sect. B 2009, 267, 1522–1525.
31. Li, S.X.; Chen, L.; Wang, M.T.; Yan, Z.Q. Effect of pre-oxidation and rare earth cerium on plasma nitriding of 42CrMo steel. Heat Treat. Met. 2021, 46, 186–189.
32. Schaaf, P. Laser nitriding of metals. Prog. Mater. Sci. 2002, 47, 1–161.
33. Chen, X.K.; Wu, G.; Wang, R.; Guo, W.T.; Yang, J.P.; Cao, S.Z.; Wang, Y.L.; Han, W.H. Laser nitriding of titanium alloy in the atmosphere environment. Surf. Coat. Technol. 2007, 201, 4843–4846.
34. Razavi, R.S.; Gordani, G.R.; Man, H.C. A review of the corrosion of laser nitrided Ti-6Al-4V. Anti-Corros. Methods Mater. 2011, 58, 140–154.
35. Fang, B.Z.; Daniel, L.; Bonakdarpour, A.; Wilkinson, D.P. Upgrading the State-of-the-Art Electrocatalysts for Proton Exchange Membrane Fuel Cell Applications. Adv. Mater. Interfaces 2022, 9, 2200349.
36. Zhao, M.M.; Huang, X.L.; Zhuang, D.M.; Sheng, L.; Xie, X.; Cao, M.; Pan, J.J.; Fan, H.Y.; He, J.P. Constructing porous nanosphere structure current collector by nitriding for lithium metal batteries. J. Energy Storage 2022, 47, 103665.
37. Arabczyk, W.; Skulmowska, K.; Pelka, R.; Lendzion-Bielun, Z. Oscillatory Mechanism of α-Fe (N)↔ γ'-Fe4N Phase Transformations during Nanocrystalline Iron Nitriding. Materials 2022, 15, 1006.

38. Sun, J.Q.; Wang, D.R.; Yang, J.; Li, F.J.; Zuo, L.L.; Ge, F.; Chen, Y.B. In Situ Preparation of Nano-Cu/Microalloyed Gradient Coating with Improved Antifriction Properties. Coatings 2022, 12, 1336.
39. Wang, Y.; Lu, S.; Zheng, J.; Liang, L. Advances in Latest Application Status, Challenges, and Future Development Direction of Electrospinning Technology in the Biomedical. J. Nanomater. 2022, 2022, 3791908.
40. Xu, W.C.; Cui, Z.D.; Zhu, S.L. Recent Advances in Open-Cell Porous Metal Materials for Electrocatalytic and Biomedical Applications. Acta Metall. Sin. 2022, 58, 1527–1544.
41. Bell, T. Source Book on Nitriding; American Society for Metals: Metals Park, OH, USA, 1977.
42. García Caballero, F.; Wang Fu, M.; Gao, M.C. Encyclopedia of Materials: Metals and Alloys; Elsevier: Amsterdam, The Netherlands, 2022.
43. Chen, W.L.; Wu, C.L.; Liu, Z.R.; Ni, S.; Hong, Y.; Zhang, Y.; Chen, J.H. Phase transformations in the nitrocarburizing surface of carbon steels revisited by microstructure and property characterizations. Acta Mater. 2013, 61, 3963–3972.
44. Wu, C.L.; Tian, L.; Hong, Y.; Wang, J.; Chen, X.Y. The effect of cooling methods and subsequent ageing on the nitrided layer of pure-iron by gas nitriding at 580 °C. J. Hunan Univ. 2015, 42, 33–39.
45. Wu, C.L.; Luo, C.P.; Zou, G.F. Phase Transformations During Composite-Chromization of steel 20. Acta Metall. Sin. 2004, 40, 1074–1078.
46. Dossett, J.L.; Totten, G.E. Introduction to steel heat treatment. Steel Heat Treat. Fundam. Process. 2013, 4, 3–25.
47. Bell, T.; Mao, K.; Sun, Y. Surface engineering design: Modelling surface engineering systems for improved tribological performance. Surf. Coat. Technol. 1998, 108, 360–368.
48. Gao, H.; Lysevych, M.; Tan, H.H.; Jagadish, C.; Zou, J. The effect of Sn addition on GaAs nanowire grown by vapor–liquid–solid growth mechanism. Nanotechnology 2018, 29, 465601.
49. Wang, B.; Sun, S.H.; Guo, M.W.; Jin, G.F.; Zhou, Z.A.; Fu, W.T. Study on pressurized gas nitriding characteristics for steel 38CrMoAlA. Surf. Coat. Technol. 2015, 279, 60–64.
50. Fare, S.; Lecis, N.; Brescia, E.; Mazzola, M. Role of grain boundaries in diffusional phenomena during gas nitriding of pure iron. Procedia Eng. 2011, 10, 2943–2948.
51. Zhao, H.; Duan, L.; Chen, G.; Fan, H.Y.; Wang, J.; Zhou, C.C. High corrosion resistance performance of 304 stainless steel after liquid nitrocarburization. Compos. Part B 2018, 155, 173–177.
52. Mirjani, M.; Mazrooei, J.; Karimzadeh, N.; Ashrafizadeh, F. Investigation of the effects of time and temperature of oxidation on corrosion behavior of plasma nitrided AISI 4140 steel. Surf. Coat. Technol. 2012, 206, 4389–4393.
53. Li, Y.; Wang, L.; Zhang, D.D.; Shen, L. The effect of surface nanocrystallization on plasma nitriding behaviour of AISI 4140 steel. Appl. Surf. Sci. 2010, 257, 979–984.
54. Miyamoto, J.; Abraha, P. The effect of plasma nitriding treatment time on the tribological properties of the AISI H13 tool steel. Surf. Coat. Technol. 2019, 375, 15–21.
55. Wang, J.; Lin, Y.H.; Yan, J.; Zen, D.Z.; Zhang, Q.A.; Huang, R.B.; Fan, H.Y. Influence of time on the microstructure of AISI 321 austenitic stainless steel in salt bath nitriding. Surf. Coat. Technol. 2012, 206, 3399–3404.
56. Arabczyk, W.; Zamlynny, J. Study of the ammonia decomposition over iron catalysts. Catal. Lett. 1999, 60, 167–171.
57. Wolowiec-Korecka, E.; Michalski, J.; Kucharska, B. Kinetic aspects of low-pressure nitriding process. Vacuum 2018, 155, 292–299.
58. Michalski, J.; Wołowiec-Korecka, E. A study of parameters of nitriding processes. Part 1. Met. Sci. Heat Treat. 2019, 61, 183–190.
59. Mitsui, H.; Kurihana, S. Solution nitriding treatment of Fe–Cr alloys under pressurized nitrogen gas. ISIJ Int. 2007, 47, 479–485.
60. Lehrer, E. Über das Eisen-Wasserstoff-Ammoniak-Gleichgewicht. Z. Elektrochem. Angew. Phys. Chem. 1930, 36, 383–392.
61. Michalski, J.; Tacikowski, J.; Wach, P.; Lunarska, E.; Baum, H. Formation of single-phase layer of γ′-nitride in controlled gas nitriding. Met. Sci. Heat Treat. 2005, 47, 516–519.
62. Nakonieczny, A.; Senatorski, J.; Tacikowski, J.; Tymowski, G.; Liliental, W. Computer Controlled Gas Nitriding—A Viable Replacement for Carburising. Heat Treat. Met. 1998, 3, 46–51.
63. Michalski, J. Characteristics and Calculations of Atmospheres for Controlled Gas Nitriding of Steel; Institute of Precision Mechanics: Warsaw, Poland, 2010.

64. Takesue, S.; Kikuchi, S.; Misaka, Y.; Morita, T.; Komotori, J. Rapid nitriding mechanism of titanium alloy by gas blow induction heating. Surf. Coat. Technol. 2020, 399, 126160.

65. Abrasonis, G.; Rivière, J.P.; Templier, C.; Muzard, S.; Pranevicius, L. Influence of surface preparation and ion flux on the nitriding efficiency of austenitic stainless steel. Surf. Coat. Technol. 2005, 196, 279–283.

66. Baranowska, J. Importance of surface activation for nitrided layer formation on austenitic stainless steel. Surf. Eng. 2010, 26, 293–298.

67. Priest, J.M.; Baldwin, M.J.; Fewell, M.P. The action of hydrogen in low-pressure rf-plasma nitriding. Surf. Coat. Technol. 2001, 145, 152–163.

68. Tong, W.P.; Tao, N.R.; Wang, Z.B.; Lu, J.; Lu, K. Nitriding iron at lower temperatures. Science 2003, 299, 686–688.

69. Lu, K.; Lu, J. Surface nanocrystallization (SNC) of metallic materials-presentation of the concept behind a new approach. J. Mater. Sci. Technol. 1999, 15, 193–197.

70. Hu, G.; Sheng, G.M.; Han, J. Investigation and Application of Surface Self Nano-crystallization Induced by Severe Plastic Deformation. Mater. Rep. 2007, 21, 117–121.

71. Azadmanjiri, J.; Berndt, C.C.; Kapoor, A.; Wen, C. Development of surface nano-crystallization in alloys by surface mechanical attrition treatment (SMAT). Crit. Rev. Solid State Mater. Sci. 2015, 40, 164–181.

72. Bahl, S.; Suwas, S.; Ungar, T.; Chatterjee, K. Elucidating microstructural evolution and strengthening mechanisms in nanocrystalline surface induced by surface mechanical attrition treatment of stainless steel. Acta Mater. 2017, 122, 138–151.

73. Jentzsch, W.D.; Böhmer, S. Investigations on nitride layer formation at the iron surface during gas nitriding. Krist. Tech. 1979, 14, 617–624.

74. Tong, W.P.; He, C.S.; He, J.C.; Zuo, L.; Tao, N.; Wang, Z. Strongly enhanced nitriding kinetics by means of grain refinement. Appl. Phys. Lett. 2006, 89, 021918.

75. Sun, J.; Tong, W.P.; Zhang, H.; Du, X.D.; Wu, Y.C. Enhanced strength and plasticity of gas nitrided iron by surface mechanical attrition pretreatment. Surf. Coat. Technol. 2016, 286, 279–284.

76. Sun, J.; Tong, W.P.; Zhang, H.; Zuo, L.; Wang, Z.B. Evaluation of surface-modified 20CrMo by plasma nitriding coupled with ion sputtering and SMAT. Surf. Coat. Technol. 2012, 213, 247–252.

77. Tong, W.P.; Han, Z.; Wang, L.M.; Lu, J.; Lu, K. Low-temperature nitriding of 38CrMoAl steel with a nanostructured surface layer induced by surface mechanical attrition treatment. Surf. Coat. Technol. 2008, 202, 4957–4963.

78. Balusamy, T.; Narayanan, T.S.N.S.; Ravichandran, K.; Park, I.S.; Lee, M.H. Plasma nitriding of AISI 304 stainless steel: Role of surface mechanical attrition treatment. Mater. Charact. 2013, 85, 38–47.

79. Lin, Y.M.; Lu, J.; Wang, L.P.; Xu, T.; Xue, Q.J. Surface nanocrystallization by surface mechanical attrition treatment and its effect on structure and properties of plasma nitrided AISI 321 stainless steel. Acta Mater. 2006, 54, 5599–5605.

80. Zhang, H.; Qin, H.F.; Ren, Z.C.; Zhao, J.Y.; Hou, X.N.; Doll, G.L.; Dong, Y.L.; Ye, C. Low-temperature nitriding of nanocrystalline Inconel 718 alloy. Surf. Coat. Technol. 2017, 330, 10–16.

81. Zhang, C.S.; Wang, Y.; Chen, D.Z.; Wu, Y.Q.; Cui, G.D.; Yang, Y.; Wang, Y.X.; Chen, Y.X. Effect of elemental doping on the catalytic activity of ABO3 perovskite oxides during low-pressure gas nitriding. Appl. Surf. Sci. 2021, 542, 148706.

82. Aleksandrov, V.A.; Ostaeva, G.Y.; Papisova, A.I.; Papisov, I.M.; Petrova, L.G.; Prikhodko, V.M.; Fatyukhin, D.S. Synthesis of copper–polymer nanocomposite on steel surface and composite-based catalyst for steel nitriding. Colloid J. 2015, 77, 556–560.

83. Dossett, J.; Totten, G.E. Fundamentals of nitriding and nitrocarburizing. In ASM Handbook: Steel Heat Treating Fundamentals and Processes; ASM International: Materials Park, OH, USA, 2013; p. 619.

84. Podgurski, H.H.; Davis, F.N. Thermochemistry and nature of nitrogen absorption in nitrogenated Fe Ti alloys. Acta Metall. 1981, 29, 1–9.

85. Steiner, T.; Mittemeijer, E.J. Alloying element nitride development in ferritic Fe-based materials upon nitriding: A review. J. Mater. Eng. Perform. 2016, 25, 2091–2102.

86. Steiner, T.; Meka, S.R.; Bischoff, E.; Waldenmaier, T.; Mittemeijer, E.J. Nitriding of ternary Fe–Cr–Mo alloys; role of the Cr/Mo-ratio. Surf. Coat. Technol. 2016, 291, 21–33.

87. Steiner, T.; Meka, S.R.; Rheingans, B.; Bischoff, E.; Waldenmaier, T.; Yeli, G.; Martin, T.L.; Bagot, P.A.J.; Moody, M.P.; Mittemeijer, E.J. Continuous and discontinuous precipitation in Fe-1 at.% Cr-1 at.% Mo alloy upon nitriding; crystal structure and composition of ternary nitrides. Philos. Mag. 2016, 96, 1509–1537.

88. Peng, T.T.; Dai, M.Y.; Cai, W.; Wei, W.; Wei, K.X.; Hu, J. The enhancement effect of salt bath preoxidation on salt bath nitriding for AISI 1045 steel. Appl. Surf. Sci. 2019, 484, 610–615.
89. Li, J.C.; Sun, F.; Wang, S.K.; Yang, X.M.; Hu, J. Catalysis effect and mechanism of pre-oxidation on direct current plasma nitriding. Trans. Mater. Heat Treat. 2014, 7, 182–186.
90. Zhen, J.Z.; Shi, Q.W.; Shi, J.; Liu, J.X. Research Progress of Low Temperature Surface Nitriding Technology for Steel Materials. Hot Work. Technol. 2019, 48, 35–40.
91. Liu, H.; Li, J.C.; Sun, F.; Hu, J. Characterization and effect of pre-oxidation on DC plasma nitriding for AISI4140 steel. Vacuum 2014, 109, 170–174.
92. Zhang, J.T.; Liu, Z.H.; Sun, J.X.; Zhao, H.L.; Shi, Q.Y.; Ma, D.W. Microstructure and mechanical property of electropulsing tempered ultrafine grained 42CrMo steel. Mater. Sci. Eng. 2020, 782, 139213.
93. Rudawska, A.; Jacniacka, E. Analysis for determining surface free energy uncertainty by the Owen–Wendt method. Int. J. Adhes. Adhes. 2009, 29, 451–457.